



# Ab initio molecular orbital calculations on chemical nature of hydrogen on surface of lithium silicate

T. Nakazawa <sup>\*</sup>, K. Yokoyama, V. Grismanovs, Y. Katano

*Japan Atomic Energy Research Institute, Tokai-mura, Naka-gun, Ibaraki-ken 319-1195, Japan*

Received 24 September 1999; accepted 15 January 2000

## Abstract

Chemical nature of superficial hydrogen on the lithium silicate and lithium silicate doped with B, Al and Ga has been investigated by ab initio molecular orbital calculations. The charge distributions and the deprotonation energy have been obtained for the model clusters:  $\text{Li}_x\text{H}_{4-x}\text{SiO}_4$  and  $\text{Li}_x\text{H}_{7-x}\text{SiAO}_7$  ( $x = 0, 1$ ; A = B, Al, Ga). It has been shown that the ionicity of surface hydrogen is strengthened by the interaction of dopant units, that operate as an electron acceptor, with surface oxygen, while it is weakened by Li atom bonded to non-bridging oxygen. Also, the deprotonation energy decreases with increasing ionicity of the superficial hydrogen. The  $\text{H}_7\text{SiAlO}_7$  cluster models have the largest ionicity of surface hydrogen and the smallest deprotonation energy among the cluster models investigated. © 2000 Elsevier Science B.V. All rights reserved.

PACS: 82.65.M; 31.15.A; 71.15.F; 68.35.B

## 1. Introduction

Several ternary lithium ceramics such as lithium silicate, zirconate, aluminate and titanate are candidates as ceramic tritium breeding materials for fusion blankets. Many reports on chemical and physical properties, irradiation and compatibility behaviors of these breeding materials have been published [1–7]. Especially, the tritium release is one of the important performances of the breeding materials.

The tritium produced with neutron irradiation mainly exists as hydroxyl groups on the surface of the breeding materials [4,7]. Thus, the tritium release process is associated with chemical properties of the hydroxyl groups on the surface. The properties of surface hydroxyl are affected by the structural changes caused due to an addition of various elements [1–3] or an irradiation [6].

Several experiments with the addition of various elements have been made for the lithium silicate to enhance the tritium release performance [1–3]. The addition of Al atoms have improved the performance for tritium release of lithium silicate [1]. However, a mechanism for this phenomenon cannot be thoroughly understood yet.

On the other hand, ab initio calculations have also been carried out for the investigation of chemical properties of surface hydroxyl groups [ $\equiv\text{Si}-\text{OH}$ ] in aluminosilicate and silica glasses [8,9]. Ab initio calculations for small discrete molecular clusters (e.g.  $\text{H}_3\text{Si}-\text{OH}$  or  $\text{H}_3\text{Si}-\text{OH}-\text{AlH}_3$ ) have indicated that substitution of Al for Si in the neighborhood of OH group leads to an increase in the ionicity of hydrogen in this group. We have also confirmed that the ionicity of superficial hydrogen in a silica network structure increases by the substitution of Al for Si with the ab initio molecular orbital calculations for larger model clusters [10]. Such substitution of trivalent metal atoms for Si influences the chemical properties of surface hydroxyl on silica glasses. The changes of chemical properties of surface hydroxyl are considered to affect the tritium release performance.

<sup>\*</sup> Corresponding author. Tel.: +81-29 282 6081; fax: +81-29 282 5460.

E-mail address: naka@maico.tokai.jaeri.go.jp (T. Nakazawa).

In the present study ab initio calculations are carried out for large molecular clusters to investigate the changes of chemical (particularly ionic) properties of surface hydroxyl groups [ $\equiv\text{Si}-\text{OH}$ ] in silica glasses wherein Si is substituted by trivalent elements, such as B, Al or Ga. The influence of lithium atom bonded to non-bridging oxygen on the properties of the surface hydroxyl group is also investigated. Effects of doping on the performance of tritium release are considered on the basis of the results obtained by the calculations.

## 2. Models and methods

Cluster models shown in Fig. 1 are employed to deduce the surface properties of pure and doped lithium silicates exposed to irradiation.  $\text{H}_4\text{SiO}_4$  and  $\text{LiH}_3\text{SiO}_4$  cluster models represent the local environments of silica glass that are formed in lithium silicate by irradiation.  $\text{H}_7\text{SiAO}_7$  and  $\text{LiH}_6\text{SiAO}_7$  cluster models (A = B, Al, Ga) are used to simulate the effect of doping in the silica glass. In the cluster models,  $\text{H}_s$  and  $\text{O}_s$  represent the surface hydrogen and oxygen atoms, respectively. Another hydrogen atoms, called 'terminators', in the cluster models are used to saturate the dangling bonds of 'surface' oxygen atoms. It has been shown that such hydrogen terminators do not affect the nature of Si–O bond [11]. Therefore, the oxygen atoms terminated by hydrogen can be considered as the bridging oxygen atoms ( $\text{O}_{br}$ ) energetically. On the other hand, the oxygen atoms adjacent to lithium atoms are regarded as non-bridging oxygen atoms ( $\text{O}_{nb}$ ). The lithium and hydrogen atoms are placed in the respective  $\text{O}_s$ –Si–O planes. For  $\text{H}_4\text{SiO}_4$  and  $\text{H}_7\text{SiAO}_7$  clusters, ideal tetrahedral environments around Si and A are also assumed with O–Si–O and O–A–O angles equal to  $109.471^\circ$ . For  $\text{H}_6\text{SiAO}_7\text{Li}$

cluster, ideal tetrahedral environments around A are only presumed with O–A–O angles equal to  $109.471^\circ$ . Within this constraint and  $C_s$  symmetry we completely optimize the structure of the cluster models. For unprotonated clusters, optimizations are limited to the distances of Si–O and O–A bonds and angle Si–O–A of main bridge in order to consider the effects of geometry relaxation of the Si–OH–A bridge on the deprotonation.

Ab initio molecular orbital calculations are carried out using the Gaussian94 program [12]. In this study, most of the calculations are done with the 6-311G\*\* basis set at the Hartree–Fock (HF) level [13]. In addition, calculations are also carried out with the 3-21G, 3-21G\*, 3-21G\*\* basis sets [13] in comparison to the results obtained with the 6-311G\*\* basis set.

The deprotonation energy (DE) of the cluster model is calculated from the difference in energy of the protonated (SH) and unprotonated ( $\text{S}^-$ ) cluster model

$$\text{DE} = E(\text{S}^-) - E(\text{SH}). \quad (1)$$

This corresponds to the energy of the reaction



i.e., the deprotonation energy of SH. Unless noted, the calculated deprotonation energies did not include zero-point energies. Atomic charges on each atom in the cluster models are obtained from a Mulliken population analysis [14].

## 3. Results and discussions

### 3.1. Geometry optimization with basis set

Table 1 lists the structural parameters for the model clusters containing no lithium atom optimized with the

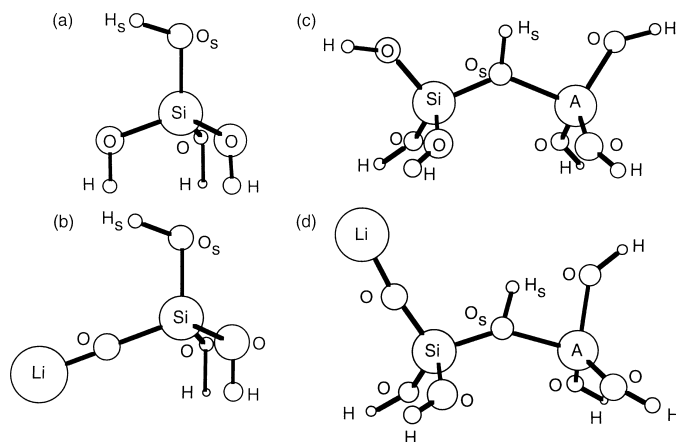


Fig. 1. Cluster modeling of the local structure of the pure and doped lithium silicate where A = B, Al, and Ga. These model clusters are used for the molecular-orbital calculations.

Table 1

Calculated molecular structure parameters at different level of theory. Bond lengths in Å and angles in degrees

| Model                             | Basic set | Bond length (Å) |       |                                |                    |                   | $\angle\text{Si-O}_{\text{br}}\text{-A}$ (°) |
|-----------------------------------|-----------|-----------------|-------|--------------------------------|--------------------|-------------------|--|
|                                   |           | Si-OH           | A-OH  | O <sub>s</sub> -H <sub>s</sub> | Si-O <sub>br</sub> | A-O <sub>br</sub> |  |
| H <sub>4</sub> SiO <sub>4</sub>   | 3-21G     | 1.638           |       | 0.954                          |                    |                   |  |
|                                   | 3-21G*    | 1.618           |       | 0.956                          |                    |                   |  |
|                                   | 3-21G**   | 1.619           |       | 0.933                          |                    |                   |  |
|                                   | 6-311G**  | 1.622           |       | 0.937                          |                    |                   |  |
| H <sub>7</sub> SiBO <sub>7</sub>  | 3-21G     | 1.615           | 1.460 | 0.973                          | 1.685              | 1.536             | 131.22                                       |
|                                   | 3-21G*    | 1.599           | 1.459 | 0.974                          | 1.670              | 1.544             | 131.33                                       |
|                                   | 3-21G**   | 1.601           | 1.459 | 0.950                          | 1.671              | 1.549             | 131.34                                       |
|                                   | 6-311G**  | 1.611           | 1.441 | 0.951                          | 1.661              | 1.564             | 133.55                                       |
| H <sub>7</sub> SiAlO <sub>7</sub> | 3-21G     | 1.611           | 1.706 | 0.974                          | 1.680              | 1.838             | 133.63                                       |
|                                   | 3-21G*    | 1.597           | 1.712 | 0.974                          | 1.667              | 1.858             | 132.72                                       |
|                                   | 3-21G**   | 1.599           | 1.711 | 0.950                          | 1.668              | 1.866             | 132.74                                       |
|                                   | 6-311G**  | 1.609           | 1.726 | 0.952                          | 1.661              | 1.904             | 136.04                                       |
| H <sub>7</sub> SiGaO <sub>7</sub> | 3-21G     | 1.609           | 1.765 | 0.972                          | 1.680              | 1.876             | 133.02                                       |
|                                   | 3-21G*    | 1.596           | 1.765 | 0.973                          | 1.663              | 1.882             | 132.86                                       |
|                                   | 3-21G**   | 1.598           | 1.806 | 0.949                          | 1.667              | 1.952             | 130.25                                       |
|                                   | 6-311G**  | 1.610           | 1.806 | 0.951                          | 1.658              | 1.997             | 134.98                                       |

HF/3-21G, HF/3-21G\*, HF/3-21G\*\* and HF/6-311G\*\* basis sets. The average experimental Si–O, B–O, Al–O and Ga–O bond lengths are 1.62 [15], 1.47 [16], 1.75 [17] and 1.82 Å [18], respectively. One can see that the calculated Si–OH, Al–OH, B–OH and Ga–OH bond lengths are in good agreement with experimental values. On the contrary, the calculated Si–O<sub>br</sub> and A–O<sub>br</sub> bond lengths are longer than the calculated Si–OH and A–OH bond lengths (A = B, Al and Ga), respectively. The difference between the bond lengths are caused by the direct interaction of A(OH)<sub>3</sub> to the oxygen of surface hydroxyl. However, the difference is not obvious from the experimental work due to the difficulty in determining the structure of surface of metal-bearing silicate (X-ray, IR and NMR studies give indirect structural information based on additional assumptions).

The average experimental Si–O<sub>br</sub>–A bond angles are 128° [19], 137° [19] and 130° [20] for A = B, Al and Ga, respectively. The calculated bond angles are in good agreement with the experimental values. The ‘non-bonded radius’ approach [21] indicates that the trend in the Si–O–A (A = B, Al, Ga) angle is generally Si–O–B angle < Si–O–Ga angle < Si–O–Al angle. The calculation with the 3-21G and 6-311G\*\* basis sets only represent the above trends for bond angles.

With respect to clusters without lithium atom, Table 2 lists DE and net atomic charges on surface hydrogen at different levels of theory. The linear relation between the DE and the charge of surface hydrogen is shown for a series of structurally related molecules, e.g. H<sub>3</sub>SiOH, H<sub>3</sub>SiOHAlH<sub>3</sub>, etc. [9]. This relation indicates that the DE decreases with an increase in the charge of surface hydrogen. The DE and the charge of surface hydrogen

Table 2

Calculated deprotonation energies and their dependence on the atomic charges on hydrogen at different level of theory

|  | H <sub>4</sub> SiO <sub>4</sub> | H <sub>7</sub> SiBO <sub>7</sub> | H <sub>7</sub> SiAlO <sub>7</sub> | H <sub>7</sub> SiGaO <sub>7</sub> |
|--|---------------------------------|----------------------------------|-----------------------------------|-----------------------------------|
| <i>Deprotonation energies</i> (kcal/mol) |                                 |                                  |                                   |                                   |
| HF/3-21G                                 | 407.27                          | 345.35                           | 334.95                            | 332.83                            |
| HF/3-21G*                                | 404.31                          | 340.97                           | 330.64                            | 257.70                            |
| HF/3-21G**                               | 412.50                          | 345.78                           | 335.26                            | 335.59                            |
| HF/6-311G**                              | 388.91                          | 326.53                           | 313.20                            | 318.72                            |
| <i>q</i> (H <sub>s</sub> )               |                                 |                                  |                                   |                                   |
| HF/3-21G                                 | 0.439                           | 0.509                            | 0.515                             | 0.513                             |
| HF/3-21G*                                | 0.425                           | 0.501                            | 0.505                             | 0.507                             |
| HF/3-21G**                               | 0.292                           | 0.381                            | 0.381                             | 0.378                             |
| HF/6-311G**                              | 0.317                           | 0.378                            | 0.400                             | 0.398                             |

are considered to be measures of the ionicity of OH bond. We can also find a linear relation between the DE and the charges of surface hydrogen calculated with the 6-311G\*\* basis sets. However, there are not the linear relations between the DE and the charges of surface hydrogen calculated with other basis sets.

Comparison of the results in Tables 1 and 2 with the experimental and theoretical results reported in other studies [8,9,14–20] shows that the 6-311G\*\* basis set is useful for prediction of geometries and properties of OH bond in the large cluster models represented by (HO)<sub>3</sub>Si(OH)A(OH)<sub>3</sub>. Nicholas et al. [8] have suggested that the structural parameters have a great sensitivity to the basis set and the cluster size. Their calculations for small clusters such as H<sub>3</sub>A(OH)AH<sub>3</sub> (A = Si, Al, B, P) have also conducted that the lower levels of theory cannot give trustworthy geometries. Therefore, the HF/

6-311G\*\* and higher levels of theory should generally be used in the ab initio calculations for large clusters such as (HO)<sub>3</sub>Si(OH)A(OH)<sub>3</sub>.

### 3.2. Atomic charge and deprotonation energy

Atomic charges on each atom in the model clusters obtained with 6-311G\*\* basis set from a Mulliken population analysis [14] are collected in Table 3. The atomic charges in Table 3 show that the surface hydrogen and oxygen in H<sub>4</sub>SiO<sub>4</sub> and LiH<sub>3</sub>SiO<sub>4</sub> cluster models are affected by the direct interaction of dopant units and the bonding of Li atom to the non-bonding oxygen.

The positive charges on surface hydrogen (H<sub>s</sub>) in H<sub>4</sub>SiO<sub>4</sub> and LiH<sub>3</sub>SiO<sub>4</sub> clusters increase by the direct interaction of dopant units. The H<sub>s</sub> in H<sub>4</sub>SiO<sub>4</sub> has the largest positive charge when the Al unit interacts with the O<sub>s</sub> in H<sub>4</sub>SiO<sub>4</sub>. The negative charges on O<sub>s</sub> in H<sub>4</sub>SiO<sub>4</sub> and LiH<sub>3</sub>SiO<sub>4</sub> become large due to interactions of the Al and Ga units with O<sub>s</sub>. On the contrary, the interactions of the B unit with O<sub>s</sub> cause the small negative charge on O<sub>s</sub> in H<sub>4</sub>SiO<sub>4</sub> and LiH<sub>3</sub>SiO<sub>4</sub>.

The changes of atomic charges on H<sub>s</sub> and O<sub>s</sub> due to their interaction with dopant units can be interpreted in terms of an electron donor–acceptor interaction [22]. The charge distributions obtained by Mulliken population analysis give electron transfers of 0.255e, 0.141e and 0.069e from H<sub>4</sub>SiO<sub>4</sub> unit to A(OH)<sub>3</sub> units (A = B, Al and Ga), respectively. The electron transfers from LiH<sub>3</sub>SiO<sub>4</sub> to A(OH)<sub>3</sub> units are also observed. The H<sub>4</sub>SiO<sub>4</sub> and LiH<sub>3</sub>SiO<sub>4</sub> units thus operate as an electron donor in cluster models. The A(OH)<sub>3</sub> units operate as an electron acceptor. By the electron donor–acceptor interaction the O<sub>s</sub> atom becomes more negative whereas the H<sub>s</sub> atom loses electrons, leading to a more ionicity of O<sub>s</sub>–H<sub>s</sub> bond in Li<sub>x</sub>H<sub>7–x</sub>SiAO<sub>7</sub> clusters as compared with the O<sub>s</sub>–H<sub>s</sub> bond in Li<sub>x</sub>H<sub>4–x</sub>SiO<sub>4</sub> clusters. The O<sub>s</sub>–H<sub>s</sub> bond thus weakens when the A(OH)<sub>3</sub> units interact with O<sub>s</sub>. The strength of this interaction is measured with the degree

of perturbation of Li<sub>x</sub>H<sub>4–x</sub>SiO<sub>4</sub> units by the A(OH)<sub>3</sub> units. The similar oxygen charges calculated for Li<sub>x</sub>H<sub>4–x</sub>SiO<sub>4</sub> and Li<sub>x</sub>H<sub>7–x</sub>SiBO<sub>7</sub> clusters (Table 3) suggest a weaker perturbation of Li<sub>x</sub>H<sub>4–x</sub>SiO<sub>4</sub> units by the B(OH)<sub>3</sub> unit on O<sub>s</sub> in comparison with perturbations by the Al(OH)<sub>3</sub> and Ga(OH)<sub>3</sub> units. Thus among the Li<sub>x</sub>H<sub>7–x</sub>SiAlO<sub>7</sub>, Li<sub>x</sub>H<sub>7–x</sub>SiGaO<sub>7</sub> and Li<sub>x</sub>H<sub>7–x</sub>SiBO<sub>7</sub> clusters, the character of the O<sub>s</sub>–H<sub>s</sub> bond in the latter ones are predicted by ab initio calculations to be closest to those in Li<sub>x</sub>H<sub>4–x</sub>SiO<sub>4</sub> clusters.

The atomic charges on each atom are also affected by the Li atom bonded to the non-bridging oxygen (Fig. 1). Due to the bonding of Li atom to the non-bridging oxygen, the positive charges on H<sub>s</sub> become smaller. The negative charges on O<sub>s</sub> in H<sub>4</sub>SiO<sub>4</sub>, H<sub>7</sub>SiAlO<sub>7</sub> and H<sub>7</sub>SiGaO<sub>7</sub> become larger by the bonding of Li atom, respectively. On the contrary, the negative charge on O<sub>s</sub> in the H<sub>7</sub>SiBO<sub>7</sub> becomes smaller. Such phenomenon is known as a ‘delocalized effect of alkali metal ion’ [23]. The non-localized effect of Na can be seen in the XPS spectra of sodium silicate glasses. That is to say, the electron delocalizations due to Li atom affect the electron density of H<sub>s</sub> and O<sub>s</sub> through the non-bridging oxygen.

On the other hand, the positive charge of Li atom in LiH<sub>3</sub>SiO<sub>4</sub> cluster increases by the interaction of dopant unit with O<sub>s</sub>. This means that the interaction of dopant units with O<sub>s</sub> influences the electron delocalization on Li atom. It can be seen from the charges of Li atoms that the electron delocalizations due to Li atom in the Al- and Ga-bearing clusters are larger than that in the B-bearing cluster. Thus, the electron delocalization on Li atom increases by the interaction of dopant units with O<sub>s</sub>. The increase in the delocalization is associated with the strength in the interaction with dopant units.

Thus, the charge of surface hydroxyl in silica and lithium silicate changes with the interaction of dopant unit and the bonding of Li atom to the non-bridging

Table 3

Mulliken atomic charges and deprotonation energies for Li<sub>x</sub>H<sub>4–x</sub>SiO<sub>4</sub> and Li<sub>x</sub>H<sub>7–x</sub>SiAO<sub>7</sub> clusters (A = B, Al, and Ga) at the HF/6-311G\*\* level

|  | Li <sub>x</sub> H <sub>4–x</sub> SiO <sub>4</sub> |        | Li <sub>x</sub> H <sub>7–x</sub> SiBO <sub>7</sub> |        | Li <sub>x</sub> H <sub>7–x</sub> SiAlO <sub>7</sub> |        | Li <sub>x</sub> H <sub>7–x</sub> SiGaO <sub>7</sub> |        |
|--|---|--------|--|--------|---|--------|---|--------|
|  | x = 0   | x = 1  | x = 0  | x = 1  | x = 0   | x = 1  | x = 0   | x = 1  |
| <i>Atomic charges</i>                    |   |        |  |        |   |        |   |        |
| q(H <sub>s</sub> )                       | +0.317  | +0.283 | +0.378   | +0.354 | +0.400  | +0.370 | +0.398  | +0.368 |
| q(O <sub>s</sub> )                       | –0.709  | –0.714 | –0.666   | –0.651 | –0.855  | –0.860 | –0.906  | –0.921 |
| q(Si)                                    | +1.645  | +1.596 | +1.682   | +1.645 | +1.736  | +1.686 | +1.723  | +1.675 |
| q(A)                                     |   |        | +0.642   | +0.635 | +1.440  | +1.444 | +1.631  | +1.641 |
| q(O <sub>nb</sub> )                      |   | –0.990 |  | –0.972 |   | –0.973 |   | –0.972 |
| q(Li)                                    |   | +0.691 |  | +0.734 |   | +0.741 |   | +0.741 |
| <i>Deprotonation energies (kcal/mol)</i> |   |        |  |        |   |        |   |        |
| DE                                       | 388.91  | 417.43 | 326.53   | 356.45 | 313.20  | 343.39 | 318.72  | 345.95 |

oxygen. The change of charge influences the strength of surface hydroxyl.

The deprotonation energy and the ionicity of  $H_s$  are considered as a measure of bond strength of surface hydroxyls [10]. For hydroxyls of different types, a linear relation between the deprotonation energy and the net charge on the proton has been found by Sauer [9]. A plot of deprotonation energies against the charges of  $H_s$  atoms is shown in Fig. 2. It can be seen that the linear relation exists between the deprotonation energies and the charges of  $H_s$ . The deprotonation energy decreases with the increase in the charge of  $H_s$ . The increase in the charge of  $H_s$  corresponds to that in the ionicity of  $H_s$ .

One can also observe in Fig. 2, that both the interaction of dopant units and the bonding of Li atom with the non-bridging oxygen influence the ionicity of  $H_s$  and the deprotonation energy. For the cluster models with or without Li atom, the trends in the ionicity of  $H_s$  are  $SiOH < Si(OH)B < Si(OH)Ga < Si(OH)Al$ . This theoretical order is in good agreement with experimental measurements for chemical properties of surface hydroxyl in isomorphously substituted forms using IR,  $^1H$  NMR [24,25]. The deprotonation energies also decrease in the order listed above, and consequently, the O–H bond weakens in the same order as well.

On the other hand, the ionicity of  $H_s$  in the cluster models with Li atom are smaller than that in the cluster models without Li atom. The deprotonation energies of the cluster models with Li atom are larger than those of the cluster models without Li atom. The  $H_7SiAlO_7$  cluster models have the largest ionicity of  $H_s$  and the smallest deprotonation energy in the investigated cluster models. The decrease in the ionicity of  $H_s$  and the increase in the deprotonation energy are due to the electron delocalization on Li atom bonded to the non-bridging oxygen.

Thus, the interaction of dopant unit with the surface oxygen increases the ionicity of  $H_s$ , and decreases the deprotonation energy. On the other hand, the bonding

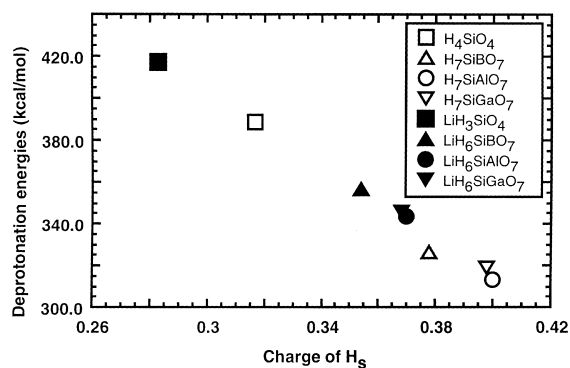


Fig. 2. Calculated deprotonation energies and their dependence on the atomic charge on hydrogen, (6-311G\*\* was used).

of Li atom to the non-bridging oxygen decreases the ionicity of  $H_s$ , and increases the deprotonation energy. That is to say, the interaction of dopant units promotes the dissociation of  $H_s$  from  $O_s$ , while the bonding of Li atom suppresses that.

### 3.3. Tritium release

Tritium release from lithium silicate is a complicated process which includes bulk diffusion and desorption from the surface. The complication of tritium release is thought to be associated with the various chemical forms of tritium on the complex surface structures due to irradiation. As the tritium has the various chemical forms, several tritium release peaks are observed in the total tritium release picture [24]. Several small release peaks observed at high temperatures ( $T > 850$  K) are considered to be associated with the bulk diffusion and the formation of  $T_2$  from  $\equiv Si-T$  and  $Li-T$ . Two large release peaks below 850 K are considered to be associated with the chemidesorption of tritiated water from surface. Almost all tritium release in the form of tritiated water originates from  $[\equiv Si-OT]$ , which is the most populated chemical form of tritium on surface of lithium silicate [4,5].

In the experiments of tritium release, the structure of  $Si-O-Si$  network formed in lithium silicate with irradiation is broken by the lithium atoms [6,26,27] because the lithium atoms are able to move easily at the elevated temperatures [28]. The number of non-bridging oxygens with Li atom increase with the break of network structure. The ab initio molecular orbital calculations for model clusters show that the Li atom bonded to non-bridging oxygen causes an increase of deprotonation energies. The increase of deprotonation energies is due to the electron delocalizations on Li atom. Thus, in the tritium release process, the tritium in the chemical form of  $[\equiv Si-OT]$  is prevented from liberation by the electron delocalizations of Li atom which exists in the neighborhood of tritium. Therefore, the electron delocalizations of Li atom are considered to be a cause of the broad and shoulder peaks which appeared in tritium release picture [24].

The chemical properties of tritium in the chemical form of  $[\equiv Si-OT]$  are investigated with the ab initio calculations for the model clusters in this study. The calculations show that the deprotonation energies decrease by the interaction of dopant units with surface oxygen. This means that the dopant atoms improve the performance of tritium release at low temperatures. Especially, the doping by Al is expected to be effective for the improvement of tritium release performance because the direct interaction of Al atom with the surface oxygen is the largest among B, Al, and Ga atoms. The results obtained in this study are consistent with the experimental results obtained by Vollath et al. [1].

#### 4. Conclusions

In this study, we present results of ab initio molecular orbital calculations on model clusters  $\text{Li}_x\text{H}_{4-x}\text{SiO}_4$  and  $\text{Li}_x\text{H}_{7-x}\text{SiAlO}_7$  ( $x = 0, 1$ ;  $A = \text{B, Al, Ga}$ ). The charge distribution and deprotonation energy are investigated on the model clusters. By the use of these clusters, the charge of surface hydrogen and deprotonation energy are shown to be influenced by the interaction of metal units with  $\text{O}_s$  and the Li atom bonded to non-bridging oxygen. The following conclusions can be drawn from this study:

1. The ionicity of  $\text{H}_s$  is strengthened by the interaction of dopant units, that operate as an electron acceptor, with  $\text{O}_s$ . On the other hand, the ionicity is weakened by the electron delocalization due to Li atom bonded to non-bridging oxygen.
2. The deprotonation energy decrease with the increase of ionicity of  $\text{H}_s$ .
3. The  $\text{H}_7\text{SiAlO}_7$  cluster models has the largest ionicity of  $\text{H}_s$  and the smallest deprotonation energy among the cluster models investigated.
4. The calculations for model clusters show that the tritium in the chemical form [ $\equiv\text{Si}-\text{OT}$ ] is easy to release by the interaction of dopant units with surface oxygen. Especially, the doping by Al is expected to be effective for the improvement of tritium release performance among B, Al and Ga atoms. On the contrary, the liberation of tritium is showed to be prevented by the electron delocalizations of Li atom which exists in the neighborhood of tritium.

#### Acknowledgements

We gratefully acknowledge the interest and the encouragement presented from Dr H. Katsuta and Dr A. Iwamoto.

#### References

- [1] D. Vollath, H. Wedemeyer, H. Zimmermann, H. Werle, J. Nucl. Mater. 174 (1990) 86.
- [2] F. Botter, J. Mouglin, B. Rasneur, S. Tistchenko, J. Kopasz, Fusion Technol. 1 (1990) 924.
- [3] M. Matsuyama, T. Takeuchi, J. Nucl. Sci. Technol. 18 (1981) 15.
- [4] A. Abramenkovs, J. Tiliks, G. Kizane, V. Grishimanovs, A. Supe, J. Nucl. Mater. 248 (1997) 116.
- [5] A.A. Abramenkovs, J.E. Tiliks, V.G. Vasiljev, Fusion Engng. Des. 17 (1991) 61.
- [6] T. Nakazawa, D. Yamaki, K. Noda, J. Nucl. Mater. 248 (1997) 121.
- [7] H. Kudo, Radiochim. Acta 50 (1990) 71.
- [8] J.B. Nicholas, R.E. Winans, R.J. Harrison, L.E. Iton, L.A. Curtiss, A.J. Hopfinger, J. Phys. Chem. 96 (1992) 10247.
- [9] J. Sauer, J. Phys. Chem. 91 (1987) 2315.
- [10] T. Nakazawa, K. Yokoyama, K. Noda, J. Nucl. Mater. 258–263 (1998) 571.
- [11] T. Uchino, T. Sakka, Y. Ogata, M. Iwasaki, J. Phys. Chem. 96 (1992) 2455.
- [12] M.J. Frisch, G.W. Trucks, H.B. Schlegel, P.M.W. Gill, B.G. Johnson, M.A. Robb, J.R. Cheeseman, T.A. Keith, G.A. Petersson, J.A. Montgomery, K. Raghavachari, M.A. Al-Laham, V.G. Zakrzewski, J.V. Ortiz, J.B. Foresman, J. Cioslowski, B.B. Stefanov, A. Nanayakkara, M. Challacombe, C.Y. Peng, P.Y. Ayala, W. Chen, M.W. Wong, J.L. Andres, E.S. Replogle, R. Gomperts, R.L. Martin, D.J. Fox, J.S. Binkley, D.J. Defrees, J. Baker, J.P. Stewart, M. Head-Gordon, C. Gonzalez, J.A. Pople, Gaussian 94, Revision D.2, Gaussian, Pittsburgh, 1995.
- [13] W.J. Hehre, L. Radom, P.v.R. Schleyer, J.A. Pople, Ab Initio Molecular Orbital Theory, Wiley, New York, 1986.
- [14] R.S. Mulliken, J. Chem. Phys. 23 (1955) 1833.
- [15] R.L. Mozzi, B.E. Warren, J. Appl. Crystallogr. 2 (1969) 164.
- [16] A.G. Pelmenschikov, G. Morosi, A. Gamba, J. Phys. Chem. 95 (1991) 10037.
- [17] J.V. Smith, S.W. Bailey, Acta Crystallogr. 16 (1963) 801.
- [18] W.H. Baur, in: M. O'Keeffe, A. Navrotsky (Eds.), Structure and Bonding in Crystals, vol. II, Academic, New York, 1982, pp. 31–52.
- [19] J.A. Tossell, G.V. Gibbs, Acta Crystallogr. A 34 (1978) 463.
- [20] J.M. Newsam, J. Phys. Chem. 92 (1988) 445.
- [21] H. He, C.F. Cheng, S. Seal, T.L. Barr, J. Klinowski, J. Phys. Chem. 99 (1995) 3235.
- [22] P. Geerlings, N. Traiel, A. Botrel, R. Lissillour, W.J. Mortier, J. Phys. Chem. 88 (1984) 5752.
- [23] T. Uchino, M. Iwasaki, T. Sakka, Y. Ogata, J. Phys. Chem. 95 (1991) 5455.
- [24] C.T-W. Chu, C.D. Chang, J. Phys. Chem. 89 (1985) 1569.
- [25] K.F.M.G.J. Scholle, A.P.M. Kentgens, W.S. Veeman, P. Frenken, G.P.M. van der Velden, J. Phys. Chem. 88 (1984) 5.
- [26] R.K. Brow, J. Vac. Sci. Technol. A 7 (1989) 1673.
- [27] T. Nakazawa, K. Noda, Y. Ishii, H. Matsui, N. Igawa, D. Vollath, H. Ohno, H. Watanabe, Fusion Technol. 2 (1992) 1444.
- [28] H. Ohno, S. Konishi, T. Nagasaki, T. Kurasawa, H. Katsuta, H. Watanabe, J. Nucl. Mater. 133&134 (1985) 181.